BMP9 inhibits the growth and migration of lung adenocarcinoma A549 cells in a bone marrow stromal cell-derived microenvironment through the MAPK/ERK and NF-κB pathways

JING WANG[1*], YAGUANG WENG[1*], MINGHAO ZHANG[2], YA LI[1], MENGTIAN FAN[1],
YANGLIU GUO[1], YANTING SUN[1], WANG LI[1] and QIONG SHI[1]

[1]Key Laboratory of Diagnostic Medicine Designated by the Chinese Ministry of Education,
Chongqing Medical University, Chongqing 400016; [2]Center for Laboratory Teaching and Management,
Chongqing Medical University, Chongqing 400016, P.R. China

Abstract. Bone is the most common distant metastatic site of lung cancer, and is particularly prone to osteolytic damage. Soluble factors secreted from bone marrow-derived cells and tumor cells contribute to the growth and metastasis of cancer cells, and enhance osteolytic damage. BMP9, as the most powerful osteogenetic factor of the bone morphogenetic protein (BMP) family, can regulate the development of various tumors. However, the effects and underlying mechanisms of BMP9 in regards to lung cancer and the bone metastatic microenvironment are poorly understood. Here, we determined the inhibitory effects of BMP9 on the proliferation and migration of lung adenocarcinoma A549 cells. When a co-culture system of A549 cells and bone marrow-derived cells (HS-5) was established, it was shown that HS-5 cells promoted the proliferation and migration of A549 cells, and metastasis and osteoclast-related factors IL-6 and IL-8 were increased in the A549 and HS-5 cells. However, BMP9 inhibited the proliferation and migration of the A549 cells in the bone microenvironment, and decreased the levels of IL-6 and IL-8. In addition, mitogen-activated protein kinase (MAPK/ERK) and nuclear factor-κB (NF-κB) signaling pathway may be involved in these effects.

Correspondence to: Dr Qiong Shi, Department of Laboratory Medicine, Chongqing Medical University, 1 Yixueyuan Road, Yuzhong, Chongqing 400016, P.R. China
E-mail: anniesq8718@aliyun.com

*Contributed equally

Introduction

Lung cancer is one of the most common malignancies and is the leading cause of cancer-related deaths worldwide. New cases of lung cancer diagnosed in the US exceed 2 million per year (1). Non-small cell lung cancer (NSCLC) accounts for 80% of lung cancer cases, including lung adenocarcinoma, squamous cell carcinoma and large-cell carcinoma (2). With surgical resection and combined-modality therapy, the overall survival has improved. However, the prognosis is still poor as most patients present with distant metastasis before being diagnosed. Therefore, almost all types of lung cancer have a poor 5-year survival rate (3). The most common metastatic site of NSCLC is bone (~30 to 40% of patients with NSCLC), followed by the brain, liver and adrenal glands (4,5). Bone lesions caused by lung cancer metastasis are often osteolytic lesions and have been associated with a poorer prognosis (6). However, the mechanisms of lung cancer metastasis to the bone resulting in osteolytic lesions remain unknown.

Paget proposed the 'seed and soil' hypothesis, which considered that tumor cells (the 'seed') have a specific affinity for the milieu of certain organs (the 'soil'). Metastases result only when the seed and soil are compatible (7). Tumor progression and metastasis are multistep processes that involve the primary tumor and distant organ microenvironment (8). Bone microenvironment homeostasis is maintained by various types of cells, such as osteoblasts, osteoclasts and bone marrow-derived mesenchymal stem cells (MSCs) (9,10). The dynamic balance is disrupted when lung cancer cells are transferred to the bone and osteolytic lesions occur. MSCs induce a tumor-suppressive effect or promote tumor growth and metastasis by secretion of a variety of cytokines, chemokines, and growth factors through a paracrine- or autocrine-mediated pathway (11-18). Some research has demonstrated that MSCs promote cell viability and this is mainly attributed to decreased apoptosis (19). Other research found that MSCs inhibited the proliferation and invasion of A549 cells *in vitro*, but favored tumor formation and growth *in vivo* (20). Therefore, the effect of MSCs on lung

cancer growth and metastasis remains controversial. However, the detailed mechanisms of the interaction of MSCs with lung cancer are largely unknown. Thus, there is an urgent need for a better understanding, as it will lead to improvements in the design of more effective therapy for lung cancer metastasis. The chemokines interleukin-6 (IL-6) and IL-8 contribute to the proliferation and metastasis of lung cancer cells or other types of cancer cells in the microenvironment of brain metastasis which are produced by astrocytes (21,22). IL-6 and IL-8 are also secreted by MSCs, and they are known to influence osteoclast formation and bone resorption (23). Whether IL-6 and IL-8 influence lung cancer progression in the bone microenvironment remains unclear.

BMPs are members of the TGF-β superfamily, which participate in the development and homeostasis of diverse tissues and organs by regulating cellular differentiation, proliferation, apoptosis and motility. BMPs are key factors in the regulation of bone formation (24). Furthermore, BMPs have been recently shown to play a pivotal role in tumor development, progression and bone metastasis (25). BMP9 has the strongest osteogenetic effect of the BMPs (26), as it has a promoting or inhibiting role in different tumor types (27-29). However, whether BMP9 affects the progression of lung cancer and osteolytic lesions of bone metastasis needs confirmation.

Based on the studies above, we aimed to investigate the effects of BMP9 on A549 cells in an HS-5 cell-mediated microenvironment, as well as the underlying mechanisms. We demonstrated that BMP9 inhibited the proliferation and metastasis, and enhanced the apoptosis of A549 cells. After the A549 cells were co-cultured with HS-5 cells, HS-5 cells promoted the proliferation, migration and invasion, and the mRNA and protein levels of IL-6 and IL-8 were increased in the HS-5 and A549 cells. However BMP9 reversed the promoting effect of the HS-5 cells. The effects were via the MAPK/ERK and NF-κB signaling pathway. These results may offer a novel strategy to efficiently inhibit the metastasis and invasion of lung cancer to the bone.

Materials and methods

Cell culture and adenoviral transfection. The human lung adenocarcinoma A549 cells and bone marrow stromal HS-5 cells were purchased from the American Type Culture Collection (ATCC; Manassas, VA, USA) and cultured in Dulbecco's modified Eagle's medium (DMEM; Hyclone, USA) containing 10% fetal bovine serum (FBS; Gibco, USA) and 1% penicillin/streptomycin at 37˚C in a 5% CO_2 incubator under humidified conditions. Recombinant adenovirus AdBMP9 and negative control AdGFP were kindly provided by Dr Tongchuan He (University of Chicago Medical Center, Chicago, IL, USA), AdBMP9 or AdGFP was transfected into the A549 or HS-5 cells with Polybrene (Sigma, USA). The medium was replaced with fresh medium after 8 h of cultivation.

Co-culture system. The co-culture system was set up using 6-well Transwell inserts (Corning, USA) with a 0.4-μm pore size. In the Transwell chamber, A549 and HS-5 cells were plated in the upper chambers at the density of 1x10^5 cells/well in 1 ml, whereas HS-5 and A549 cells were plated in 6-well plates at the density of 2x10^5 cells/well in 2 ml. Cells became adherent after 6 h, and then were placed together in DMEM supplemented with 2% FBS for 3 days. Cells alone were used as the control.

Cell proliferation assay. Cell viability was detected by MTT [3-(4, 5-dimethylthiazol-2-yl)-2,5-diphenyltetrazolium bromide] assay. A total of 4x10^4 A549 cells/well were cultured in 6-well plates and 2x10^4 HS-5 cells were cultured in a chamber. The A549 cells were treated with AdGFP or AdBMP9, and the cells were cultured for 24, 48 and 72 h. At the indicated time, MTT reagent (Sigma) was added (200 μl/well), and incubation was carried out at 37˚C for 4 h. Next, 3 ml of dimethyl sulfoxide (DMSO) was added to the 6-well plates to dissolve the formazan product for 10 min at room temperature, and 150 μl lysate was added into the 96-well plate. Finally, the absorbance was measured at 492 nm using a microplate reader. Each group was conducted in quintuplicate, and the overall experiment was repeated 3 times.

Colony-forming assay. Log-phase A549 cells treated with AdGFP or AdBMP9 were collected and seeded in 10% FBS medium at 200 cells/well in 6-well plates for 14 days. When clones were observed, the cells were washed twice with PBS and stained with 1% crystal violet. The colony formation rate was calculated as: (Colony number/seeded cell number) x 100%. Each experiment was repeated thrice.

Flow cytometry. Cell apoptosis analysis was assessed by flow cytometry. The A549 cells were seeded into 6-well plates at a density of 2x10^5 cells/well and treated with AdGFP or AdBMP9 for 48 h. Then the cells were harvested and re-suspended in 1 ml cold PBS, and samples were added with propidium iodide (PI) and FITC-Annexin V for cell apoptosis analysis according to the manufacturer's protocol (Invitrogen, USA). Respectively, data were analyzed using FACS Sorter (Becton Dickinson, San Jose, CA, USA).

Wound-healing assay. A549 cells were seeded into 6-well plates and HS-5 cells were seeded into chambers. A549 cells were treated with AdGFP or AdBMP9. When A549 cells had grown to 95% confluency, the monolayer was scratched with a sterile pipette tip, and then washed with PBS twice to remove cellular debris. Culture medium was replaced with fresh DMEM containing 1% FBS, and then co-cultured with the HS-5 cells. Cells that migrated into the scratched area were compared using bright field microscopy at 48 h. Experiments were performed in triplicate.

Transwell invasion assay. HS-5 cells are seeded into a 24-well plate containing 10% FBS. After the cells became adherent, the A549 cells (4x10^4/400 μl) in FBS-free DMEM were seeded into the chambers (24-well Transwell chambers, 8-μm pore size; Corning). The Transwell membrane was coated with 1:3 diluted Matrigel (Sigma) beforehand. After 24 h, the cells that invaded to the underside of the filter were fixed with 4% paraformaldehyde and stained with 0.1% crystal violet, and counted by bright field microscopy. All the experiments were repeated 3 times.

Table I. The sequences of the siRNAs.

siRNAs	Sense	Antisense
siIL-6	#1: AGACAUGUAACAAGAGUAA	UCUGUACAUUGUUCUCAUU
	#2: AAACAACCUGAACCUUCCA	UUUGUUGGACUUGGAAGGU
	#3: GGAGACUUGCCUGGUGAAA	CCUCUGAACGGACCACUUU
siIL-8	#1: GCCAAGGAGUGCUAAAGAA	CGGUUCCUCACGAUUUCUU
	#2: GCGCCAACACAGAAAUUAU	CGCGGUUGUGUCUUUAAUA
	#3: CAAAGAACUGAGAGUGAUU	GUUUCUUGACUCUCACUAA

Table II. The sequences of the primers for RT-PCR.

Genes	Primer sequence (5'-3')	Product size (bp)
GAPDH	F: CAGCGACACCCACTCCTC	120
	R: TGAGGTCCACCACCCTGT	
BMP9	F: CTGCCCTTCTTTGTTGTCTT	322
	R: CCTTACACTCGTAGGCTTCATA	
IL-6	F: TAGTGAGGAACAAGCCAGAG	234
	R: TACATTTGCCGAAGAGCC	
IL-8	F: ACTCCAAACCTTTCCACC	155
	R: CTTCTCCACAACCCTCTG	

F, forward; R, reverse.

RNA interference. A549 cells were seeded into 6-well plates and incubated at 37°C in a CO_2 incubator until they were 60-80% confluent, then the cells were transfected with 50 nM IL-6 or IL-8 siRNA according to the manufacturer's instructions. Transfected cells were incubated for 3 days. The siRNA sequences which aimed to target IL-6 and IL-8 were designed by RiboBio and are shown in Table I.

RNA isolation and relative quantitative RT-PCR. A549 cells were co-cultured with HS-5 cells or alone or were treated with AdBMP9 in FBS-free DMEM for 3 days. Total RNA was extracted using TRIzol reagent (Invitrogen, Carlsbad, CA, USA) according to the manufacturer's protocol. Total RNA (2 μg) was used for cDNA synthesis by reverse transcriptase-PCR. The mRNA expression was quantitatively determined using a real-time polymerase chain reaction (PCR) system (Bio-Rad, USA) using SYBR Green PCR Master Mix. GAPDH was used as the invariant control. Amplification was performed with the following protocol: denaturation at 94°C for 30 sec, annealing at 55°C for 30 sec, and extension at 72°C for 50 sec. The primer sequences used for real-time PCR are shown in Table II.

Western blot analysis. A549 cells were cultured alone or co-cultured with HS-5 cells, and treated with AdBMP9 for 3 days. Then the A549 cells were washed three times with cold PBS and lysed in RIPA lysis buffer, and the cell lysate was denatured after boiling. The protein concentration was measured by a BCA protein assay kit. Fifty micrograms of lysate was loaded onto 10% SDS-PAGE gels, and subsequently transferred onto PVDF membranes. After blocking with 5% bovine serum albumin (BSA; Solarbio) in TBST for 2 h at 37°C, the membranes were incubated with the following primary antibodies [polyclonal rabbit anti-BMP9 (Abcam, Cambridge, MA, USA); anti-caspase3, anti-Bax, anti-Bcl2, anti-MMP2, anti-PCNA, anti-IL-6, anti-IL-8 (Wanleibio, Shenyang, China); monoclonal rabbit anti-ERK1/2, anti-p-ERK1/2, anti-P38, anti-p-P38, anti-AKT, anti-p-AKT, anti-p-P65 (Cell Signaling Technology, Danvers, MA, USA); monoclonal mouse anti-β-actin (ZSGBBIO, Beijing, China); rabbit anti-histone (Abmart, Shanghai, China)] at 4°C overnight, washed with TBST for 3 times, followed by incubation with a secondary antibody conjugating with horseradish peroxidase (ZSGBBIO) for 1 h, and washed again. Protein levels were quantified with the SuperSignal West Pico Chemiluminescent Substrate kit.

Animal studies. The animal experiments were performed in accordance with the guidelines established by the Animal Care and Use Committee of Chongqing Medical University Laboratory Animal Research. The 4- to 6-week-old male NOD/SCID mice were randomly divided into 4 groups (n=4/group), respectively, and were injected subcutaneously with A549 cells ($6x10^6$); a mixture of A549 ($6x10^6$) and HS-5 cells ($3x10^6$); A549/GFP ($6x10^6$) and HS-5 cells ($3x10^6$); A549/BMP9 ($6x10^6$) and HS-5 cells ($3x10^6$). Tumor volume was measured every week with Vernier calipers, and calculated in mm^3 as $ab^2/2$, where 'a' and 'b' represent the largest and smallest tumor diameter, respectively. The mice were sacrificed after 7 weeks, and tumor tissues were collected, embedded in paraffin, and cut into 4-μm sections. The sections were stained using H&E and immunohistochemical analyses were conducted.

Immunohistochemical staining for Ki-67. Paraffin sections of tumor tissues were de-waxed, rehydrated and heat-treated for antigen retrieval with citric acid buffer. The sections were then blocked with normal goat serum for 30 min, incubated with polyclonal rabbit anti-Ki-67 (Wanleibio) at 4°C overnight, and were analyzed using an immunohistochemistry kit (PV-9001; ZSGBBIO) following the manufacturer's protocol. Staining procedures were performed under standardized conditions. The sections were counterstained with hematoxylin, mounted, and coverslipped. Staining intensity was independently assessed by the authors.

Statistical analysis. All values are expressed as the mean ± SEM. Statistical significance was determined using

the Student's t-test in GraphPad Prism 5. A P-value of <0.05 was considered to indicate a statistically significant result.

Results

Overexpression of BMP9 inhibits the proliferation, migration and invasion, and promotes the apoptosis of A549 cells. We aimed to ascertain the effect of BMP9 on the biological behavior of NSCLC cells AdBMP9 was used to overexpress BMP9 in the lung adenocarcinoma A549 cells which have a low level of BMP9. The infection effciency of AdBMP9 in the A549 cells was observed under a fluorescence microscope (Fig. 1A). RT-PCR and western blot results showed that these recombinant cells were successfully established (P<0.001; Fig. 1B and C). Cell proliferation ability was assessed by MTT and colony-forming assays. The results showed that the proliferation of the A549/BMP9 cells was decreased significantly (Fig. 2A and B). The cell apoptosis rate of the A549/BMP9 cells was significantly increased compared with the rates noted in the blank and GFP groups by flow cytometry (P<0.01; Fig. 2C). Cell migration and invasion abilities were detected by wound-healing and Transwell invasion assays. The findings demonstrated that BMP9 decreased the wound-healing rate and the number of invasive A549 cells (Fig. 2D and E). Furthermore, we detected the protein levels of DNA replication factor (PCNA), cell apoptosis factors (pro-apoptosis factors caspase-3 and Bax and anti-apoptosis factor Bcl2), and migration-related factor (MMP-2) by western blotting. The results showed that PCNA, MMP-2 and Bcl2 were decreased, while caspase-3 and Bax were upregulated by BMP9 overexpression in the A549 cells (Fig. 2F).

HS-5 cells stimulate the proliferation, migration and invasion of A549 cells, and BMP9 inhibits the malignant phenotype of A549 cells in a co-culture system. When co-cultured with HS-5 cells, the cell viability of the A549 cells obviously increased as determined by MTT assay. Cell migration and invasion abilities were increased as determined by wound-healing and Transwell invasion assays (Fig. 3A-C). After AdBMP9 was added to the co-culture system, the cell proliferation rate, the wound-healing rate and the number of invading A549 cells in the co-culture/BMP9 group was found to be significantly decreased than these values in the co-culture/GFP group (Fig. 3A-C). To investigate the effects of HS-5 cells and BMP9 on the tumor growth of lung cancer cells *in vivo*, A549 or adenovirus-infected A549 cells and HS-5 cells were subcutaneously implanted into nude mice. The tumor size was monitored weekly and the tumors were dissected after xenografting for 7 weeks. Tumor volumes differed obviously after 4 weeks. HS-5 cells accelerated the growth of the A549 tumors, while BMP9 significantly inhibited the accelerative role of the HS-5 cells compared to the GFP group (Fig. 3D). These results were consistent with those *in vitro*. H&E staining showed no variation in heterogeneity between the single A549 and A549/HS-5 group, but there were many lymphocytic invasive cells in the tumor tissue of the BMP9 group (Fig. 3E). Ki-67 expression was detected by immunohistochemical staining. The results showed that the Ki-67-positive cell rate was increased in the A549/HS-5 group when compared with the A549 group, and BMP9 inhibited the expression of Ki-67 (Fig. 3F).
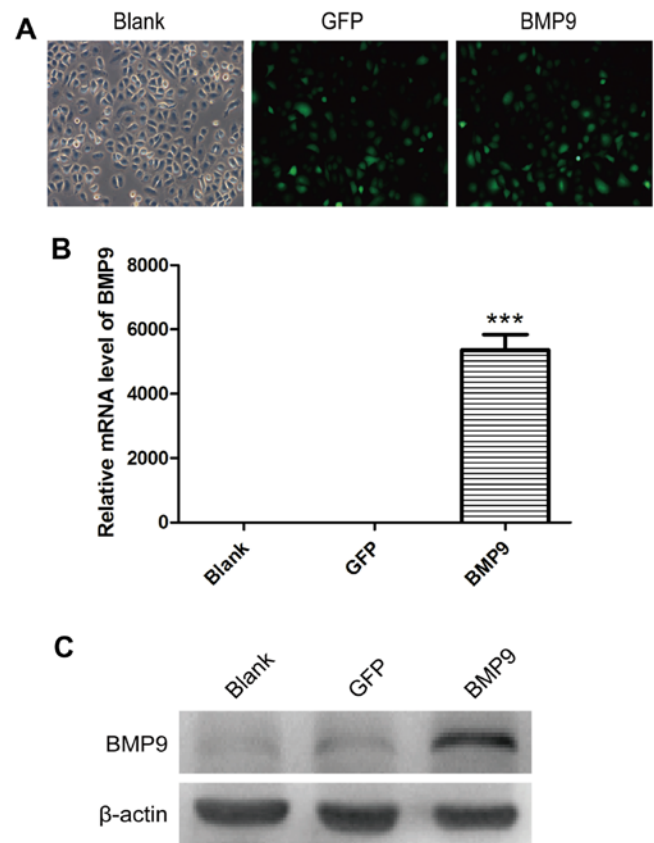

Figure 1. Overexpression of BMP9 was confirmed in A549 cells following infection with recombinant adenovirus BMP9 (AdBMP9). (A) Infection effciency of the A549 cells infected with AdGFP and AdBMP9 for 24 h observed under a fluorescence microscope (x100 magnification). (B and C) Expression of BMP9 in the A549 cells was analyzed by RT-PCR and western blot analysis after infection with AdBMP9 (***P<0.001 as compared with GFP).

IL-6 and IL-8 expression levels are increased in the A549 and HS-5 cells in the co-culture system. Studies have reported that expression levels of IL-6 and IL-8 are higher in lung cancer patients with metastasis than those without metastasis. Meanwhile, IL-6 and IL-8 could be secreted by bone marrow stromal cells, and they are known to influence osteoclast formation and bone resorption. BMP9 is the most effective bone formation factor of the BMPs. We investigated whether IL-6 and IL-8 are related to the pro-metastatic effect of A549 cells in the HS-5 cell-mediated tumor microenvironment. We detected the mRNA and protein levels of IL-6 and IL-8 in the A549 and HS-5 cells in the co-culture system by RT-PCR and western blotting. IL-6 and IL-8 were increased in the A549 (Fig. 4A and B) and HS-5 cells (Fig. 4C and D, but had no statistical significance) in the co-culture system, BMP9 inhibited the expression levels of IL-6 and IL-8 compared to the GFP group (Fig. 4A-C). When IL-6 and IL-8 were knocked down by siRNA, the interference efficiency of the three siRNAs targeting IL-6 and IL-8 was verified by RT-PCR and western blotting (Fig. 4E and F). IL-6-siRNA-3 and IL-8-siRNA-2 were the most highly functional one and were used in the following assays. The wound-healing rate and the number of invasive A549 cells were decreased in the co-culture system with knockdown of IL-6 or IL-8 (Fig. 4G and H).
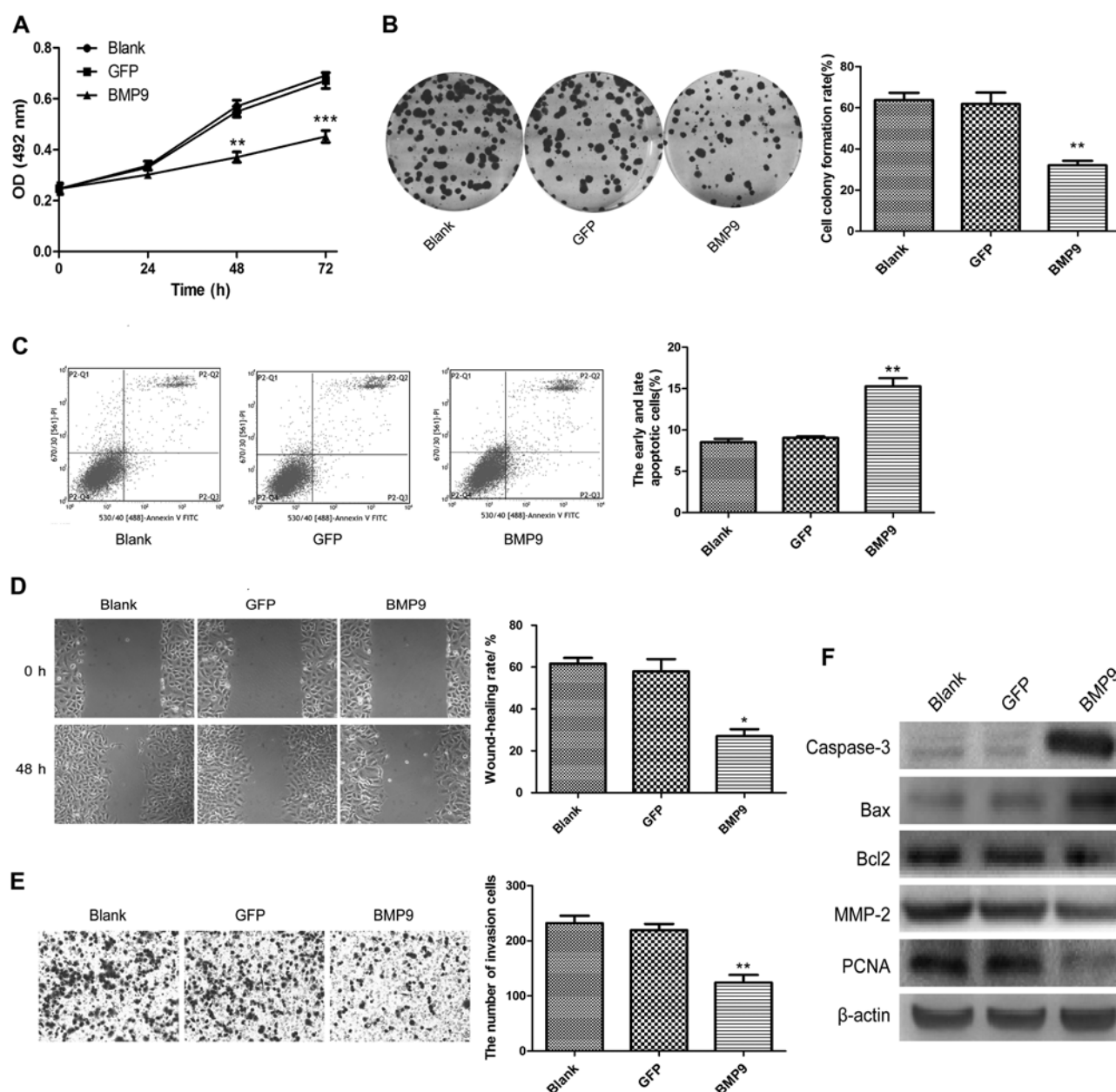
Figure 2. Overexpression of BMP9 inhibited cell proliferation, migration, and invasion, and induces apoptosis in A549 cells. (A and B) Cell proliferation was detected by MTT and colony forming assays. (C) Cell apoptosis was measured by flow cytometry. (D and E) Cell migration and invasion were measured by wound-healing and Transwell assays (x100 magnification). (F) The expression levels of cell apoptosis factors (caspase-3, Bax, Bcl2), migration-related factor (MMP-2), DNA replication factor (PCNA) were detected by western blot analysis. Data are shown as mean ± SD of 3 individual measurements ($^{*}P<0.05$, $^{**}P<0.01$, $^{***}P<0.001$ as compared with GFP).

Effects of IL-6 and IL-8 on A549 cells via the MAPK/ERK1/2 and NF-κB signaling pathways. NF-κB and MAPK are crucial signaling pathways responsible for gene induction in NSCLC cell proliferation (30,31). Activation of these pathways in lung cancer cells initiates signaling cascades and leads to overproduction of inflammatory cytokines and growth factors including IL-6, IL-8 and MMPs, which promote cancer progression and metastasis (32,33). Whether these pathways involved in lung cancer cells thrive within the bone environment remains unkown. As shown in Fig. 5A and B, the A549 cells had enhanced expression of p-ERK1/2 and p-P65, but not p-P38 and p-AKT after co-culture with the HS-5 cells for 3 days. When IL-6 and IL-8 were silenced by small interference RNA siIL-6 and siIL-8, or overexpres-

sion of BMP9, the expression of p-ERK1/2 and p-P65 was decreased. The same results were found with the MEK- and NF-κB-specific inhibitors U0126 (10 μM; Selleckchem, USA) and BAY11-7082 (5 μM; Beyotime, Shanghai, China), respectively (Fig. 5C and D). Meanwhile, U0126 and BAY11-7082 decreased the invasive ability of the A549 cells in the co-culture system (Fig. 5E).

Discussion

Bone is the most common metastatic site of metastatic non-small cell lung cancer (4). NSCLC patients with bone metastasis have a poor prognosis, which is due to skeletal-related events, such as pathological fractures, spinal cord compression and
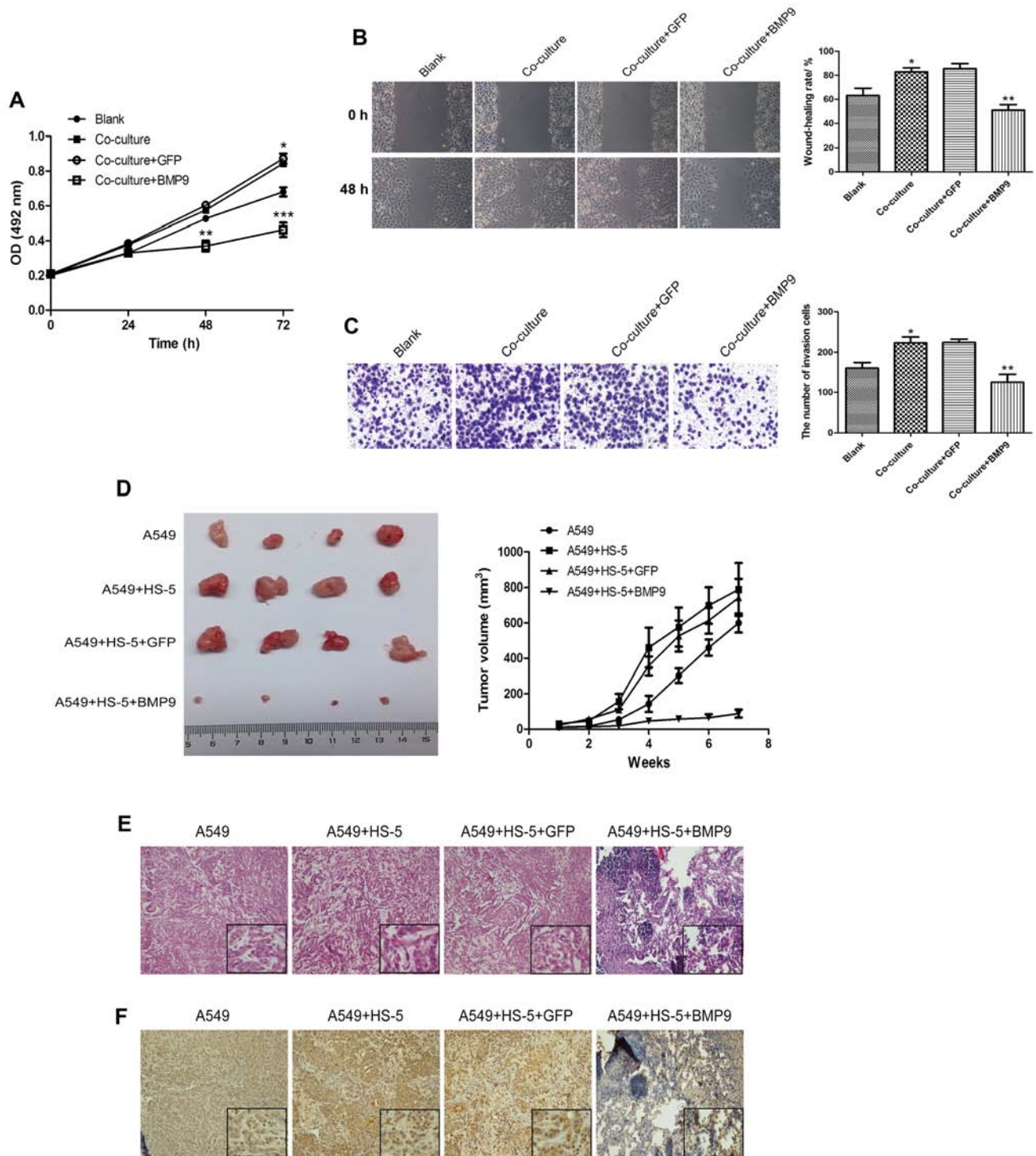
Figure 3. HS-5 cells promoted the growth of A549 cells *in vitro* and *in vivo*, and increased migration and invasion of A549 cells *in vitro*. BMP9 inhibited the promoting role of the HS-5 cells. (A-C) Cell proliferation, migration and invasion were detected by MTT, wound-healing and Transwell assays. (D) The tumor sizes and tumor growth curves in the various groups. (E) H&E staining of tumor tissues (x100 magnification). (F) Ki-67 staining of the various groups by immunohistochemical staining (x100 magnification). Data are shown as mean ± SD of three individual measurements ($^{*}P<0.05$, $^{**}P<0.01$, as compared with blank or co-culture/GFP).

hypercalcemia of malignancy (34,35). Bone marrow-derived cells are one of the important tumor stroma components in the tumor microenvironment (36). Bone marrow-derived cells promote the development of lung cancer micrometastases by releasing extracellular matrix (ECM)-bound growth factors such as IL-6, IL-8, PTHrp, which also promote osteolytic

lesions. And this vicious cycle is regulated by the NF-κB signaling pathway (37).

BMPs have been reported to have important effects on many tumor types. In lung cancer, BMP2 upregulation was found to increase the incidence and influence the prognosis of lung cancer patients (38). The expression of BMP5 was
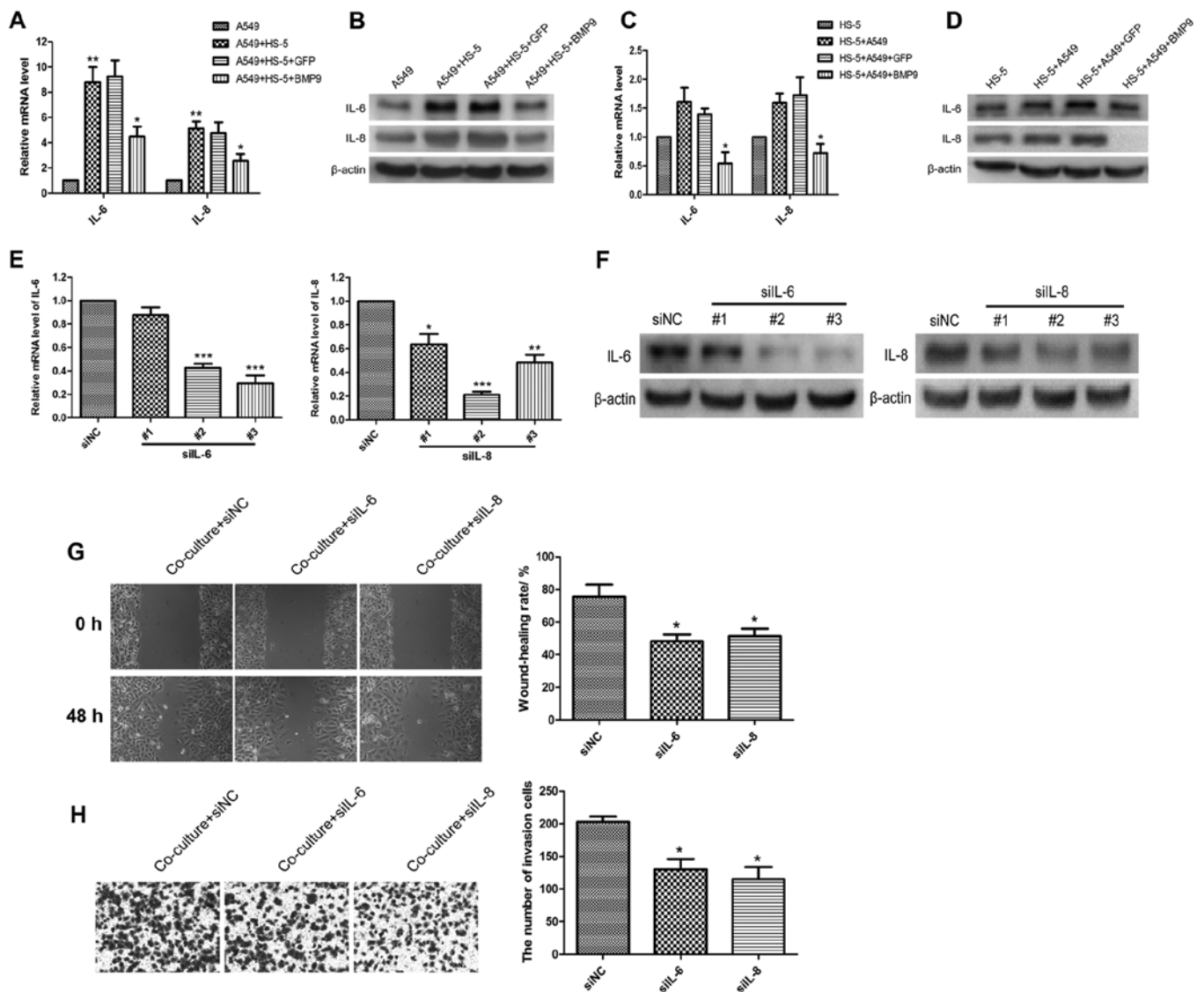
Figure 4. Expression levels of IL-6 and IL-8 were increased in A549 cells after co-culturing with HS-5 cells, BMP9 inhibited the expression of IL-6 and IL-8. Knockdown of IL-6 and IL-8 by siRNA inhibited the migration and invasion of the A549 cells. (A-D) mRNA and protein levels of IL-6 and IL-8 in the A549 and HS-5 cells were analyzed by RT-PCR and western blot analysis. (E and F) Expression of IL-6 and IL-8 in the A549 cells was detected by RT-PCR and western blot analysis after transfection with siRNA for 48 h. (G and H) Cell migration and invasion were measured by wound-healing and Transwell assays after knockdown of IL-6 and IL-8. Data are shown as mean ± SD of three individual measurements (*P<0.05, **P<0.01, ***P<0.001 as compared with the A549 or A549+HS-5+GFP or HS-5 or HS-5+A549+GFP or siNC group).

found to be downregulated in lung cancer tissues and may serve as a potential prognostic biomarker or therapeutic target for NSCLC (39). BMP9 is the most effective BMP in bone formation. It has been reported that it can promote the growth of ovarian cancer cells, inhibit the growth and invasion of prostate cancer PC-3 cells, and enhance apoptosis, and repress the invasion and migration of breast cancer cells (27,28,40). BMP9 was also found to inhibit the invasion of breast cancer MDA-MB-231 cells and reduce osteolytic lesions in a bone marrow stromal cell-mediated tumor microenvironment (29). However, the role of BMP9 in lung cancers, particularly in bone metastasis of lung cancers, requires further investigation.

To study the role of BMP9 in lung cancer, particularly in the bone microenvironment of lung cancer, we chose lung adenocarcinoma A549 cells which have low expression of BMP9, and established BMP9-overexpressing A549 cells by infection with recombinant adenovirus AdBMP9. *In vitro*, we

found that BMP9 inhibited the growth, migration and invasion, and promoted the apoptosis of A549 cells. The growth, migration and invasion were increased in A549 cells after being co-cultured with HS-5 cells. However, BMP9 also reversed these biological activities in the tumor microenvironment. The *in vivo* experiment indicated that HS-5 cells increased tumor growth and BMP9 reversed the promoting effect of HS-5 cells. We detected whether the chemokines IL-6 and IL-8 are involved in regulating the progression of lung cancer in the bone microenvironment. The data determined that the levels of IL-6 and IL-8 were increased in the A549 and HS-5 cells when they were co-cultured. BMP9 decreased the expression of IL-6 and IL-8. When IL-6 and IL-8 were downregulated by siRNAs in the co-culture system, the migration and invasion of the A549 cells were decreased. The results indicated that IL-6 and IL-8 are associated with the migration and invasion of A549 cells in the tumor microenvironment, and BMP9 has
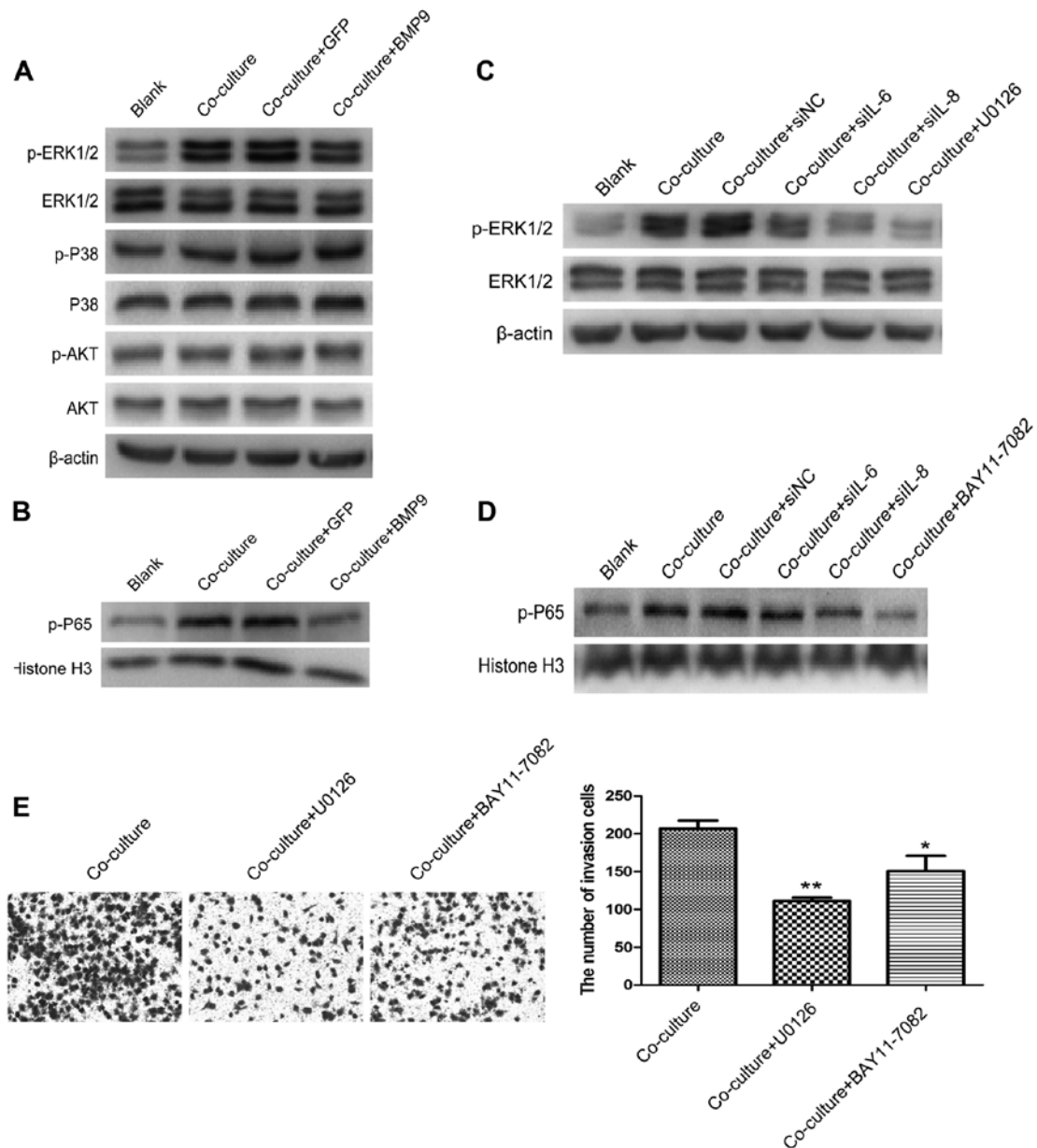
Figure 5. Effects of HS-5 cells and BMP9 on MAPK-ERK and NF-κB activation in human A549 cells. (A) The p-ERK1/2 level was increased in the A549 cells, but not p-P38 and p-AKT after co-culture with the HS-5 cells, and BMP9 reversed the increase in p-ERK1/2 as analyzed by western blot analysis. (B) The p-P65 level in the nuclei was increased in the A549 cells after co-culture with HS-5 cells, and BMP9 reversed the increase. (C and D) p-ERK1/2 and p-P65 levels were decreased in the A549 cells treated with siIL-6 and siIL-8. (E) Invasive ability of the A549 cells treated with U0126 and BAY11-7082 was downregulated as measured by Transwell invasion assay (*P<0.05, **P<0.01, as compared with co-culture).

an inhibitory role in lung cancer progression and osteolytic lesions. In order to further elucidate the correlative mechanisms of IL-6, IL-8 and BMP9 with lung cancer progression, we detected interleukin and BMP-related MAPK, PI3K/AKT and NF-κB signaling pathways (31,41). Our data showed that the MAPK/ERK and NF-κB signaling pathways were activated in co-cultured A549 cells which had high expression of IL-6 and IL-8. siIL-6 and siIL-8 inhibited the activation of the MAPK/ERK and NF-κB signaling pathways, and had the same effect with BMP9.

In conclusion, the study showed that MSCs can promote the proliferation, migration and invasion of A549 cells. This promoting role may be mediated by IL-6 and IL-8 via the MAPK/ERK and NF-κB signaling pathways. BMP9 regulated the crosstalk between A549 and HS-5 cells in the co-culture system, which inhibited the proliferation and migration of A549 cells.

Acknowledgements

References

1. Siegel R, Ma J, Zou Z and Jemal A: Cancer statistics, 2014. CA Cancer J Clin 64: 9-29, 2014.
2. D'Addario G and Felip E; ESMO Guidelines Working Group: Non-small-cell lung cancer: ESMO clinical recommendations for diagnosis, treatment and follow-up. Ann Oncol 20 (Suppl 4): 68-70, 2009.
3. Siddiqui S, Ali MU, Ali MA, Shah N and Nasreen S: Lung carcinoma: Its profile and changing trends. J Ayub Med Coll Abbottabad 22: 116-119, 2010.
4. Tamura T, Kurishima K, Nakazawa K, Kagohashi K, Ishikawa H, Satoh H and Hizawa N: Specific organ metastases and survival in metastatic non-small-cell lung cancer. Mol Clin Oncol 3: 217-221, 2015.
5. Coleman RE: Metastatic bone disease: Clinical features, pathophysiology and treatment strategies. Cancer Treat Rev 27: 165-176, 2001.
6. Tubiana-Hulin M: Incidence, prevalence and distribution of bone metastases. Bone 12 (Suppl 1): S9-S10, 1991.
7. Paget S: The distribution of secondary growths in cancer of the breast. 1889. Cancer Metastasis Rev 8: 98-101, 1989.
8. Langley RR and Fidler IJ: Tumor cell-organ microenvironment interactions in the pathogenesis of cancer metastasis. Endocr Rev 28: 297-321, 2007.
9. Sivasubramaniyan K, Lehnen D, Ghazanfari R, Sobiesiak M, Harichandan A, Mortha E, Petkova N, Grimm S, Cerabona F, de Zwart P, et al: Phenotypic and functional heterogeneity of human bone marrow- and amnion-derived MSC subsets. Ann NY Acad Sci 1266: 94-106, 2012.
10. Baksh D, Song L and Tuan RS: Adult mesenchymal stem cells: Characterization, differentiation, and application in cell and gene therapy. J Cell Mol Med 8: 301-316, 2004.
11. Gomes CM: The dual role of mesenchymal stem cells in tumor progression. Stem Cell Res Ther 4: 42, 2013.
12. Sung SY, Hsieh CL, Law A, Zhau HE, Pathak S, Multani AS, Lim S, Coleman IM, Wu LC, Figg WD, et al: Coevolution of prostate cancer and bone stroma in three-dimensional coculture: Implications for cancer growth and metastasis. Cancer Res 68: 9996-10003, 2008.
13. Windus LC, Glover TT and Avery VM: Bone-stromal cells up-regulate tumourigenic markers in a tumour-stromal 3D model of prostate cancer. Mol Cancer 12: 112, 2013.
14. Goldstein RH, Reagan MR, Anderson K, Kaplan DL and Rosenblatt M: Human bone marrow-derived MSCs can home to orthotopic breast cancer tumors and promote bone metastasis. Cancer Res 70: 10044-10050, 2010.
15. Karnoub AE, Dash AB, Vo AP, Sullivan A, Brooks MW, Bell GW, Richardson AL, Polyak K, Tubo R and Weinberg RA: Mesenchymal stem cells within tumour stroma promote breast cancer metastasis. Nature 449: 557-563, 2007.
16. Hernanda PY, Pedroza-Gonzalez A, van der Laan LJ, Bröker ME, Hoogduijn MJ, Ijzermans JN, Bruno MJ, Janssen HL, Peppelenbosch MP and Pan Q: Tumor promotion through the mesenchymal stem cell compartment in human hepatocellular carcinoma. Carcinogenesis 34: 2330-2340, 2013.
17. Mizuguchi T, Hui T, Palm K, Sugiyama N, Mitaka T, Demetriou AA and Rozga J: Enhanced proliferation and differentiation of rat hepatocytes cultured with bone marrow stromal cells. J Cell Physiol 189: 106-119, 2001.
18. Song B, Kim B, Choi SH, Song KY, Chung YG, Lee YS and Park G: Mesenchymal stromal cells promote tumor progression in fibrosarcoma and gastric cancer cells. Korean J Pathol 48: 217-224, 2014.
19. Zhang MH, Hu YD, Xu Y, Xiao Y, Luo Y, Song ZC and Zhou J: Human mesenchymal stem cells enhance autophagy of lung carcinoma cells against apoptosis during serum deprivation. Int J Oncol 42: 1390-1398, 2013.
20. Tian LL, Yue W, Zhu F, Li S and Li W: Human mesenchymal stem cells play a dual role on tumor cell growth in vitro and in vivo. J Cell Physiol 226: 1860-1867, 2011.
21. Seike T, Fujita K, Yamakawa Y, Kido MA, Takiguchi S, Teramoto N, Iguchi H and Noda M: Interaction between lung cancer cells and astrocytes via specific inflammatory cytokines in the microenvironment of brain metastasis. Clin Exp Metastasis 28: 13-25, 2011.
22. Sierra A, Price JE, García-Ramirez M, Méndez O, López L and Fabra A: Astrocyte-derived cytokines contribute to the metastatic brain specificity of breast cancer cells. Lab Invest 77: 357-368, 1997.
23. Kudo O, Sabokbar A, Pocock A, Itonaga I, Fujikawa Y and Athanasou NA: Interleukin-6 and interleukin-11 support human osteoclast formation by a RANKL-independent mechanism. Bone 32: 1-7, 2003.
24. Wang RN, Green J, Wang Z, Deng Y, Qiao M, Peabody M, Zhang Q, Ye J, Yan Z, Denduluri S, et al: Bone Morphogenetic Protein (BMP) signaling in development and human diseases. Genes Dis 1: 87-105, 2014.
25. Ye L, Lewis-Russell JM, Kyanaston HG and Jiang WG: Bone morphogenetic proteins and their receptor signaling in prostate cancer. Histol Histopathol 22: 1129-1147, 2007.
26. Luu HH, Song WX, Luo X, Manning D, Luo J, Deng ZL, Sharff KA, Montag AG, Haydon RC and He TC: Distinct roles of bone morphogenetic proteins in osteogenic differentiation of mesenchymal stem cells. J Orthop Res 25: 665-677, 2007.
27. Ye L, Kynaston H and Jiang WG: Bone morphogenetic protein-9 induces apoptosis in prostate cancer cells, the role of prostate apoptosis response-4. Mol Cancer Res 6: 1594-1606, 2008.
28. Wang K, Feng H, Ren W, Sun X, Luo J, Tang M, Zhou L, Weng Y, He TC and Zhang Y: BMP9 inhibits the proliferation and invasiveness of breast cancer cells MDA-MB-231. J Cancer Res Clin Oncol 137: 1687-1696, 2011.
29. Wan S, Liu Y, Weng Y, Wang W, Ren W, Fei C, Chen Y, Zhang Z, Wang T, Wang J, et al: BMP9 regulates cross-talk between breast cancer cells and bone marrow-derived mesenchymal stem cells. Cell Oncol (Dordr) 37: 363-375, 2014.
30. Alam M, Wang JH, Coffey JC, Qadri SS, O'Donnell A, Aherne T and Redmond HP: Characterization of the effects of cyclooxygenase-2 inhibition in the regulation of apoptosis in human small and non-small cell lung cancer cell lines. Ann Surg Oncol 14: 2678-2684, 2007.
31. Zhao J, Harper R, Barchowsky A and Di YP: Identification of multiple MAPK-mediated transcription factors regulated by tobacco smoke in airway epithelial cells. Am J Physiol Lung Cell Mol Physiol 293: L480-L490, 2007.
32. Kausar H, Jeyabalan J, Aqil F, Chabba D, Sidana J, Singh IP and Gupta RC: Berry anthocyanidins synergistically suppress growth and invasive potential of human non-small-cell lung cancer cells. Cancer Lett 325: 54-62, 2012.
33. Lemmon CR, Woo JH, Tully E, Wilsbach K and Gabrielson E: Nuclear factor-kappaB (NF-kappaB) mediates a protective response in cancer cells treated with inhibitors of fatty acid synthase. J Biol Chem 286: 31457-31465, 2011.
34. Bauml J, Mick R, Zhang Y, Watt CD, Vachani A, Aggarwal C, Evans T and Langer C: Determinants of survival in advanced non--small-cell lung cancer in the era of targeted therapies. Clin Lung Cancer 14: 581-591, 2013.
35. Saad F, Lipton A, Cook R, Chen YM, Smith M and Coleman R: Pathologic fractures correlate with reduced survival in patients with malignant bone disease. Cancer 110: 1860-1867, 2007.
36. El-Nikhely N, Larzabal L, Seeger W, Calvo A and Savai R: Tumor-stromal interactions in lung cancer: Novel candidate targets for therapeutic intervention. Expert Opin Investig Drugs 21: 1107-1122, 2012.
37. Peng X, Guo W, Ren T, Lou Z, Lu X, Zhang S, Lu Q and Sun Y: Differential expression of the RANKL/RANK/OPG system is associated with bone metastasis in human non-small cell lung cancer. PLoS One 8: e58361, 2013.
38. Fei ZH, Yao CY, Yang XL, Huang XE and Ma SL: Serum BMP-2 up-regulation as an indicator of poor survival in advanced non-small cell lung cancer patients. Asian Pac J Cancer Prev 14: 5293-5299, 2013.
39. Deng T, Lin D, Zhang M, Zhao Q, Li W, Zhong B, Deng Y and Fu X: Differential expression of bone morphogenetic protein 5 in human lung squamous cell carcinoma and adenocarcinoma. Acta Biochim Biophys Sin (Shanghai) 47: 557-563, 2015.
40. Herrera B, van Dinther M, Ten Dijke P and Inman GJ: Autocrine bone morphogenetic protein-9 signals through activin receptor-like kinase-2/Smad1/Smad4 to promote ovarian cancer cell proliferation. Cancer Res 69: 9254-9262, 2009.
41. Mu Y, Gudey SK and Landström M: Non-Smad signaling pathways. Cell Tissue Res 347: 11-20, 2012.